Article

Current-Mode Active Filter Using EX-CCCII

Montree Kumngern [1] , Fabian Khateb [2,3,4,*] , Tomasz Kulej [5] and Siraphop Tooprakai [1]

1   Department of Telecommunications Engineering, School of Engineering, King Mongkut's Institute of Technology Ladkrabang, Bangkok 10520, Thailand; montree.ku@kmitl.ac.th (M.K.); sirapop.to@kmitl.ac.th (S.T.)
2   Department of Microelectronics, Brno University of Technology, Technická 10, 601 90 Brno, Czech Republic
3   Faculty of Biomedical Engineering, Czech Technical University in Prague, nám. Sítná 3105, 272 01 Kladno, Czech Republic
4   Department of Electrical Engineering, Brno University of Defence, Kounicova 65, 662 10 Brno, Czech Republic
5   Department of Electrical Engineering, Czestochowa University of Technology, 42-201 Czestochowa, Poland; kulej@el.pcz.czest.pl
*   Correspondence: khateb@vutbr.cz

Abstract: This paper presents a novel multiple-input and multiple-output current-mode universal analog filter with electronic tuning capability. The proposed circuit uses a single second-generation current-controlled current conveyor with extra-X terminals (EX-CCCII) and two grounded capacitors. The filter can offer five standard filtering functions, namely low-pass, high-pass, band-pass, band-stop, all-pass responses, in the same circuit without changing the internal configuration of the filter by selecting appropriate input and output signals. To obtain the five standard filtering functions, inverted input signal and input matching conditions are absent. The natural frequency of all filter responses can be electronically controlled. The proposed circuit was simulated by SPICE using 0.18 µm CMOS process from Taiwan Semiconductor Manufacturing Company (TSMC). The results of experiments using the integrated circuit operational amplifier AD844 confirm the functionality of the new filter.

Keywords: extra-x second-generation current-controlled current conveyor (EX-CCCII); current-mode circuit; active filter; analog circuit

1. Introduction

In many circuit designs, a second-generation current conveyor (CCII) is utilized to realize analog signal processing circuits, especially current-mode signal processing circuits. The circuits using CCII as an active element offer higher linearity, better signal bandwidth, and wider dynamic range compared to the operational amplifier (op-amp) based circuits [1,2]. Moreover, CCII is simpler to implement compared to the op-amp structure. There are many CCII structures available in literature [3–15]. In [3], a conventional CCII that has three terminals (the y-, x-, z-terminals) is proposed. This CCII provides the characteristics of $V_y = V_x$, $I_x = I_z$, a high resistance at the y- and z-terminals (ideally infinite), and a low resistance at the x-terminal (ideally zero). In practice, however, the resistance at the x-terminal is not equal to zero as it exhibits a parasitic resistance. In [4], a current-controlled CCII (CCCII) is introduced. Due to the CCCII, the parasitic resistance at the x-terminal (R_x) can be used as a parameter for filter application and this R_x can be electronically controlled. Moreover, the CCCII-based circuit does not contain a passive resistor. Note that the CCCII still has a single x-terminal, like the CCII.

Recently, the extra x-terminal CCII (EX-CCII) has been introduced [5]. This device is an enhancement of the conventional CCII, which increases the number of x- and z-terminals. Figure 1 shows the electrical symbol of the conventional CCII and the EX-CCII. Compared with the conventional CCII in Figure 1a, the EX-CCII in Figure 1b has extra x-input terminals and z-output terminals. The characteristics of the EX-CCII can be given by

$V_y = V_{x1} = V_{x2}$, $I_{x1} = I_{z1}$, and $I_{x2} = I_{z2}$. In addition, the number of x-input terminals and z-output terminals of the EX-CCII can be increased to any number. Thus, the EX-CCII is a versatile and flexible active device. There are many applications of the EX-CCII available in literature, including precision rectifiers [6–9], fractional-order controllers [10–12], digital modulators [13], analog multipliers [14], wave signal generators [15], first-order filters [16,17], and universal filters [18]. It is worth noting that the EX-CCII based circuit does not provide electronic tuning capability.
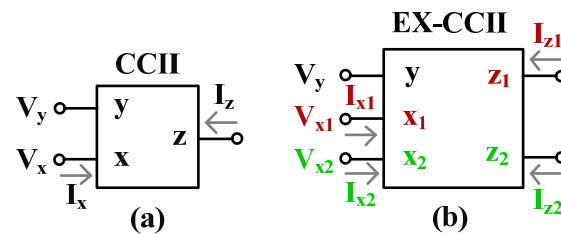
Figure 1. Electrical symbol of (**a**) a conventional CCII and (**b**) an EX-CCII.

If the parasitic resistance at the x-terminal of the EX-CCII is considered, then the circuit becomes EX-CCCII and its parasitic resistances at the x-terminals can be used as an adjustable parameter. This is advantageous for applications such active filters and oscillators. The EX-CCCII can be used for applications such as oscillators [19–23], instrumentation amplifiers [24,25], immittance simulators [26], precision rectifiers [27], first-order filters [28–30], and universal filters [31–34]. This work focuses on the EX-CCCII based universal filter. Considering the universal filters in [31–34], these filters suffer from some drawbacks. First, in order to obtain the five filtering functions (i.e., the low-pass filter (LPF), high-pass filter (HPF), band-pass filter (BPF), band-stop filter (BSF), and all-pass filter (APF)), the filters use inverted input signals and require input matching condition [31–34]. Second, the filters use passive component matching conditions [34]. The use of a single EX-CCCII based filter, made possible through the use of the current-mode technique, is advantageous in these universal filters [31–34]. Note that the realization of signal addition and subtraction in current-mode circuits is easier than for their voltage-mode counterparts.

This work proposes a single EX-CCCII-based current-mode universal filter. It is a multiple-input and multiple-output filter providing five standard filtering functions, namely low-pass, high-pass, band-pass, band-stop, and all-pass functions, that can be obtained by selecting appropriate input and output terminals. The proposed filter offers the following advantages: (i) it uses a single EX-CCCII; (ii) it does not require inverted input signals or the fulfilment of input matching conditions to realize the five standard filtering functions; (iii) it does not require matching of passive components; (iv) it offers electronic tuning capability of a natural frequency.

The rest of this paper is organized as follows: Section 2 provides a description of the proposed EX-CCCII and the proposed current-mode universal filter. Sections 3 and 4 present the simulation and experimental results, respectively. Section 5 concludes the paper.

2. Circuit Description

This section contains four subsections, where the first subsection introduces the second generation current-controlled current conveyor with extra-x terminal that is used for realizing the proposed filter. The second subsection introduces the proposed current-mode universal filter, while the non-ideal gain analysis and non-ideal parasitic analysis are presented in the third and fourth subsections, respectively.

2.1. Second-Generation Current-Controlled Current Conveyor with Extra-X Terminal

Figure 2a shows the electrical symbol of the EX-CCCII and Figure 2b shows the equivalent circuit. The input voltage present at the y-terminal is conveyed to the x_1- and x_2-

terminals. R_{x1} and R_{x2} are the parasitic resistances at the x_1- and x_2-terminals, respectively, that can be controlled by the DC biasing current.
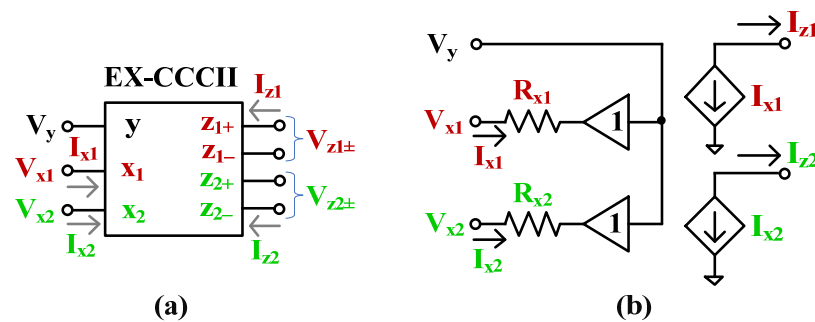

Figure 2. EX-CCCII (**a**) electrical symbol, (**b**) equivalent circuit.

The input current at the x_1- and x_2-terminals is conveyed to the z_1- and z_2-terminals, respectively. The minus-type output of the z_1- and z_2-terminals can easily be obtained using a cross-coupled current mirror topology. Thus, the port relationships of the ideal EX-CCCII shown in Figure 2a can be given by

$$\begin{pmatrix} I_y \\ V_{x1} \\ V_{x2} \\ I_{z1} \\ I_{z2} \end{pmatrix} = \begin{pmatrix} 0 & 0 & 0 & 0 & 0 \\ 1 & R_{x1} & 0 & 0 & 0 \\ 1 & 0 & R_{x2} & 0 & 0 \\ 0 & \pm 1 & 0 & 0 & 0 \\ 0 & 0 & \pm 1 & 0 & 0 \end{pmatrix} \begin{pmatrix} V_y \\ I_{x1} \\ I_{x2} \\ V_{z1} \\ V_{z2} \end{pmatrix} \tag{1}$$

The CMOS structure of the EX-CCCII in Figure 2a is shown in Figure 3. The circuit is based on complementary source followers, current mirrors, and cross coupled current mirrors. The complementary source follower is a dual translinear loop (M_1, M_2, M_4, M_5) and (M_1, M_3, M_4, M_6) where the gate-source voltages V_{GS} of the NMOS transistors (M_1, M_2 and M_3) and PMOS transistors (M_4, M_5 and M_6) are to match. In these loops, the input voltage V_y is transferred to the outputs of the follower V_{x1} and V_{x2} precisely; if the drain currents of M_1, M_4 equal to the drain currents of M_2, M_5 and M_3, M_6 and vice versa, the drain current of M_1, M_4 is transferred precisely to M_2, M_5 and M_3, M_6 if the input and output voltages and the gate-source voltages of the respective transistors and their size are equal. The current mirrors (M_9, M_{10}, M_{14}, M_{15}, M_{21}, M_{22}, M_{26}, M_{27}) are used to transfer the x terminals current to their respective z+ terminals. The cross coupled current mirrors (M_{11}–M_{13}, M_{16}–M_{18}, M_{23}–M_{25}, M_{28}–M_{30}) are used to transfer the x+ terminals current to their respective negative z- terminals. The biasing circuit realized by the transistors M_b, M_7, M_8, M_{19}, M_{20} and the biasing current source I_{set} provides all reference currents in the circuit.
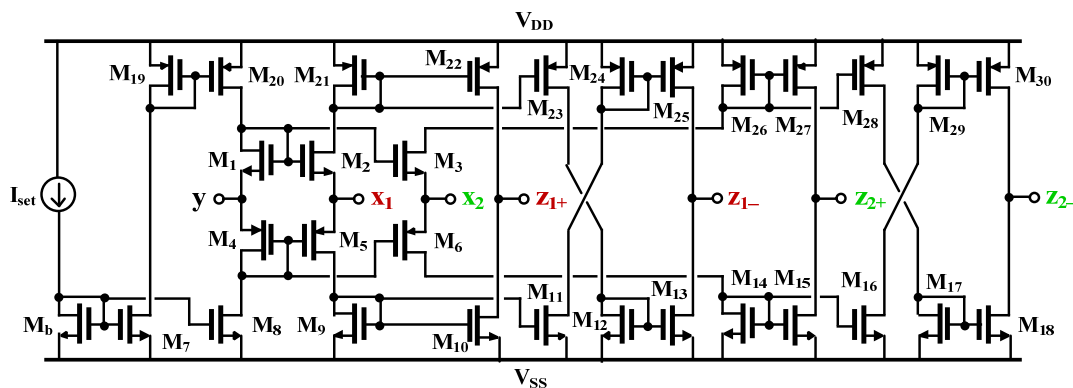

Figure 3. CMOS structure of EX-CCCII.

Considering a dual translinear loop, the parasitic resistances R_{x1} and R_{x2} at the x_1- and x_2-terminals, respectively, can be expressed [32] by

$$R_{x1} = R_{x2} = \frac{1}{\sqrt{2I_{set}C_{ox}}\left(\sqrt{\mu_p \left(\frac{W}{L}\right)_p} + \sqrt{\mu_n \left(\frac{W}{L}\right)_n}\right)} \tag{2}$$

where I_{set} is the biasing current, C_{ox} is the oxide capacitance per unit area, μ_p and μ_n are the mobility of the holes and electrons, respectively, $(W/L)_p$ is the ratio of width to length of the channels of M_5–M_6, and $(W/L)_n$ is the ratio of width to length of the channels of M_2–M_3. From (2), the parasitic resistances R_{x1} and R_{x2} can be controlled by the biasing current I_{set}. These resistors have the same resistance values.

The input current at the x_1-terminal is conveyed to the z_{1+}-terminal by the current mirrors M_7–M_8, M_{19}–M_{20}, and the input current at x_2 is conveyed to z_{2+} by the current mirrors M_{12}–M_{13}, M_{24}–M_{24}. The minus-type outputs z_{1-} and z_{2-} can be implemented using the cross-coupled current mirror topology. Additional copies of these $z_{+,-}$ outputs can be obtained using the cascade structure for these terminals.

2.2. Current-Mode Universal Filter Using EX-CCCII

Figure 4a shows the proposed current-mode universal filter, and the block diagram that corresponds to Figure 4a is shown in Figure 4b. It is based on one lossless integrator and one lossy integrator loop. It employs one EX-CCCII and two grounded capacitors. Thanks to the extra x-terminal and multiple-outputs of the EX-CCCII, the filter is realized with only one active block. The circuit has four input currents (I_1, I_2, I_3, I_4) and three output currents (I_{o1}, I_{o2}, I_{o3}). Using (1) and nodal analysis, the outputs of the circuit in Figure 4a is given by

$$I_{o1} = \frac{D(s)I_3 + I_2 - (sC_2R_{x2} + 1)I_1}{D(s)} \tag{3}$$

$$I_{o2} = \frac{D(s)I_4 - sC_1R_{x1}I_2 + I_1}{D(s)} \tag{4}$$

$$I_{o3} = \frac{-sC_1R_{x1}I_2 + I_1}{D(s)} \tag{5}$$

where $D(s) = s^2C_1C_2R_{x1}R_{x2} + sC_1R_{x1} + 1$.
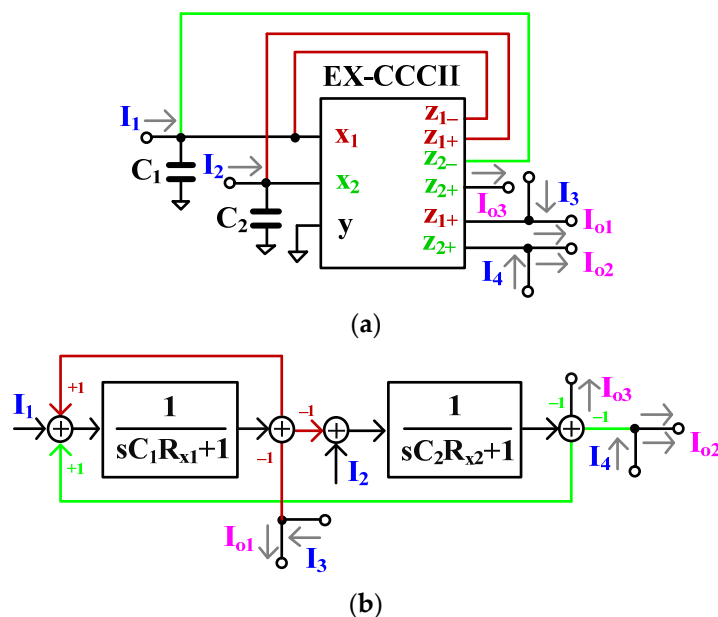

(a)

(b)

Figure 4. (**a**) Proposed current-mode universal filter using EX-CCCII, (**b**) its block diagram.

From (3)–(5), the variant filtering functions of the low-pass filter (LPF), high-pass filter (HPF), band-pass filter (BPF), band-stop filter (BSF), and all-pass filter (APF) can be obtained, as shown in Table 1. For Table 1, it should be noted that the input terminal that is not selected to supply input signals can be floating, while the output terminal that is not selected to supply output signals should be grounded.

Table 1. Variant filtering functions.

Filtering Function		Input	Output
LPF	Non-inverting	I_2	I_{o1}
	Non-inverting	I_1	I_{o2} or I_{o3}
BPF	Inverting	I_2	I_{o2} or I_{o3}
HPF	Non-inverting	$I_1 = I_3$	I_{o1}
BSP	Non-inverting	$I_2 = I_4$	I_{o2}
	Non-inverting	$I_1 = I_3$	$I_{o1} + I_{o2}$
APF	Non-inverting	$I_2 = I_4$	$I_{o2} + I_{o3}$

The natural frequency (ω_o) and the quality factor (Q) of all filter responses are given by

$$\omega_o = \frac{1}{\sqrt{C_1 C_2 R_{x1} R_{x2}}} \tag{6}$$

$$Q = \sqrt{\frac{C_1 R_{x1}}{C_2 R_{x2}}} \tag{7}$$

From Table 1, it is evident that the circuit does not need an inverted input signal, i.e., $-I_{\text{in}}$, and double input signal, i.e., $2I_{\text{in}}$, to realize all filtering functions.

From (6), we can see that the natural frequency can be controlled electronically by R_{x1} and R_{x2} through the biasing current I_{set}. The quality factor, as shown in (7), is given by C_1/C_2 while maintaining $R_{x1} = R_{x2}$.

2.3. Non-Ideal Gain Analysis

Taking the errors of the EX-CCCII into account, the relationship of the terminal voltages and currents can be written by

$$\left.\begin{array}{l} V_{xj} = \alpha_j V_y \\ I_{zj} = \beta_j I_{xj} \end{array}\right\} \tag{8}$$

where α_j is the voltage gain from y-terminal to x_j-terminal, and $\beta_{j\pm}$ is the current gain from $x_{j\pm}$-terminals to $z_{j\pm}$-terminals (j = 1, 2). Ideally, α_j and $\beta_{j\pm}$ should be equal to 1. However, in practice, these unity gains will be affected by the voltage and current tracking errors. These can be expressed by $\beta_{j\pm} = (1 - \varepsilon_{jv\pm})$ and $\alpha_{j\pm} = (1 - \varepsilon_{ji\pm})$, where $\varepsilon_{jv\pm}$ is the voltage tracking error and $\varepsilon_{ji\pm}$ is the current tracking error.

Taking into account the nonidealities of the EX-CCCII, the denominator of the non-ideal current-mode universal filter's transfer functions can expressed by

$$\begin{array}{l} D(s) = s^2 C_1 C_2 R_{x1} R_{x2} + s(C_1 R_{x1} + C_2 R_{x2}(1 - \beta_{1-}\beta_{1+})) \\ \qquad\qquad + (\beta_{1-}\beta_{1+}\beta_{2+} + (1 - \beta_{1-}\beta_{1+})) \end{array} \tag{9}$$

The parameters ω_o and Q of the non-ideal filter are given by

$$\omega_o = \sqrt{\frac{\beta_{1-}\beta_{1+}\beta_{2+} + (1 - \beta_{1-}\beta_{1+})}{C_1 C_2 R_{x1} R_{x2}}} \tag{10}$$

$$Q = \frac{\sqrt{(\beta_{1-}\beta_{1+}\beta_{2+} + (1 - \beta_{1-}\beta_{1+}))C_1 C_2 R_{x1} R_{x2}}}{C_1 R_{x1} + C_2 R_{x2}(1 - \beta_{1-}\beta_{1+})} \tag{11}$$

The non-ideal gains of the EX-CCCII will slightly change the values of ω_o and Q.

2.4. Non-Ideal Parasitic Analysis

The non-ideal model of the EX-CCCII is shown in Figure 4. The terminals x_1 and x_2 have low resistances R_{x2} and R_{x2}, respectively. The parasitic inductances in series with them are ignored. The terminals y, $z_{1\pm}$, and $z_{2\pm}$ are shunted by parallel connections of parasitic resistances and capacitances, $R_y//C_y$, $R_{z1\pm}//C_{z1\pm}$, $R_{z2\pm}//C_{z2\pm}$.

Considering the EX-CCCII parasitics, the denominator of the transfer functions can be expressed by

$$D(s) = s^2 C_1' C_2' R_{x1} R_{x2} + s C_1' R_{x1} \left(1 + \frac{C_2' R_{x1} R_{x2} G_a + C_1' R_{x1} R_{x2} G_b}{C_1' R_{x1}}\right) + (R_{x1} R_{x2} G_a G_b + R_{x1} G_a) + 1 \tag{12}$$

where $C_1' = C_1 + C_{z1-} + C_{z2-}$, $C_2' = C_2 + C_{z1+}$, $G_a = 1/(R_{z1-}//R_{z2-})$, $G_b = 1/R_{z1+}$.

Letting

$$\left.\begin{array}{r}\frac{C_2' R_{x1} R_{x2} G_a + C_1' R_{x1} R_{x2} G_b}{C_1' R_{x1}} = 0 \\ R_{x2} G_a G_b + R_{x1} G_a = 0\end{array}\right\} \tag{13}$$

which is possible if R_{z1-}, R_{z2-}, R_{z1+} are very high resistances compared with R_{x1}, R_{x2}, the parameters ω_o and Q of the non-ideal current-mode universal filter can be expressed by

$$\omega_o = \frac{1}{\sqrt{C_1' C_2' R_{x1} R_{x2}}} \tag{14}$$

$$Q = \sqrt{\frac{C_1' R_{x1}}{C_2' R_{x2}}} \tag{15}$$

The parasitic capacitances will affect the parameters ω_o and Q of the filter and their impact can be minimized by choosing $C_1 \gg C_{z1-} + C_{z2-}$, $C_2 \gg C_{z1+}$.

3. Simulation Results

The proposed current-mode analog filter was designed and simulated in SPICE using TSMC 0.18 μm CMOS technology (Taiwan Semiconductor Manufacturing Company (TSMC), Hsinchu, Taiwan). The aspect ratios of the transistors are shown in Table 2. The supply voltage was ±0.5 V. The summarized performance of the designed EX-CCCII is shown in Table 3 [32].

Table 2. Aspect ratios for the transistors in the EX-CCCII.

Transistor	W/L (μm/μm)
M_1, M_2, M_3	5/0.36
M_4, M_5, M_6	10/0.36
M_b, M_7–M_{18}	3/0.36
M_{19}–M_{30}	6/0.36

Figure 5 shows the simulated parasitic resistance at the x-terminal (R_x) when the biasing current I_{set} was varied from 2 to 50 μA. When the biasing current was increased from 2 to 50 μA, the observed parasitic resistance R_x decreased from 20.32 to 2.29 kΩ.

Table 3. Parameters of the designed EX-CCCII.

Parameters	Value
Supply voltage	± 0.5 V
Technology	0.18 μm
DC voltage range	-100 mV to 100 mV
Voltage gain	0.953
Current gain I_{z+}/I_x I_{z-}/I_x	1.01 1.04
-3 dB bandwidth VF	0.502 GHz
-3 dB bandwidth CF I_{z+}/I_x I_{z-}/I_x	141.9 MHz 121.4 MHz
R_x (I_{set} = 2–60 μA)	20.3 kΩ–2.29 kΩ
$R_y//C_y$	100 kΩ//0.251 pF
$R_z//C_z$	462 kΩ//0.051 pF
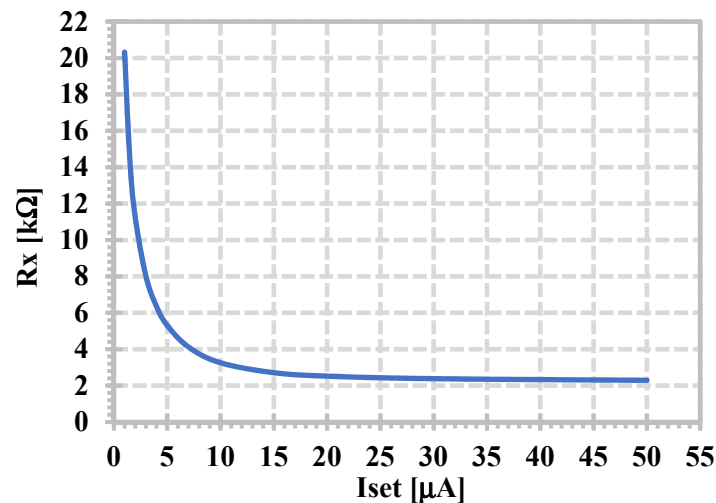
Figure 5. Simulated parasitic resistance R_x with different I_{set}.

Figure 6 shows the simulated magnitude and phase frequency responses of the LPF, HPF, BPF, and BSF with $C_1 = C_2 = 20$ pF and $I_{set} = 20$ μA. Figure 7 shows the simulated magnitude and phase frequency responses of the APF. The filters offer a 3.23 MHz of the natural frequency. Thus, it is evident from Figures 6 and 7 that the proposed current-mode filter can realize the five standard filtering functions in the same circuit without inverted input signal requirements.

The tuning capability of the proposed current-mode filter was tested by varying the bias current I_{set}. The simulated magnitude frequency response is shown in Figure 8. The natural frequency was (0.724, 1.51, 3.47) MHz when the bias current I_{set} was (2, 5, 40) μA, respectively.

The LPF was used to test the linearity of the proposed current-mode filter. The input signal has an in-band frequency of 10 kHz and the amplitude was varied. Figure 9 shows the simulated total harmonic distortion (THD) of the current-mode filter when the input amplitude was varied. The THD was 1.038% when the amplitude was 70 μA (140 μA$_{P-P}$). Figure 10 shows the equivalent output current noise of the LPF. The integrated current noise over the bandwidth of 3.23 MHz was calculated to be 17.13 nA, giving a dynamic range of 69.2 dB.
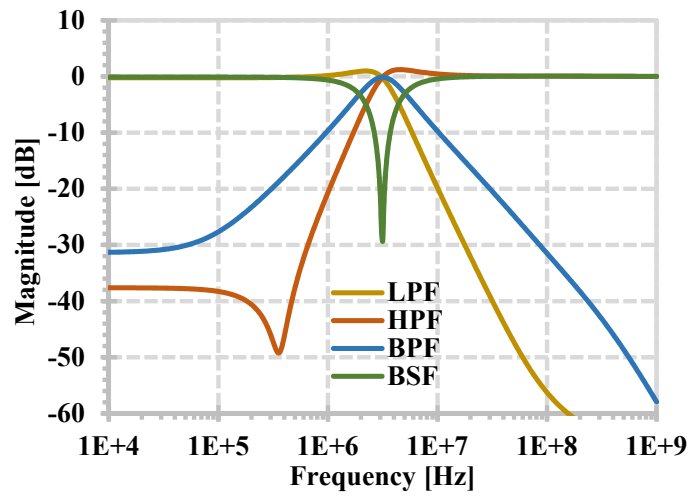
Figure 6. Simulated magnitude and phase frequency responses of the LPF, HPF, BPF, and BSF.
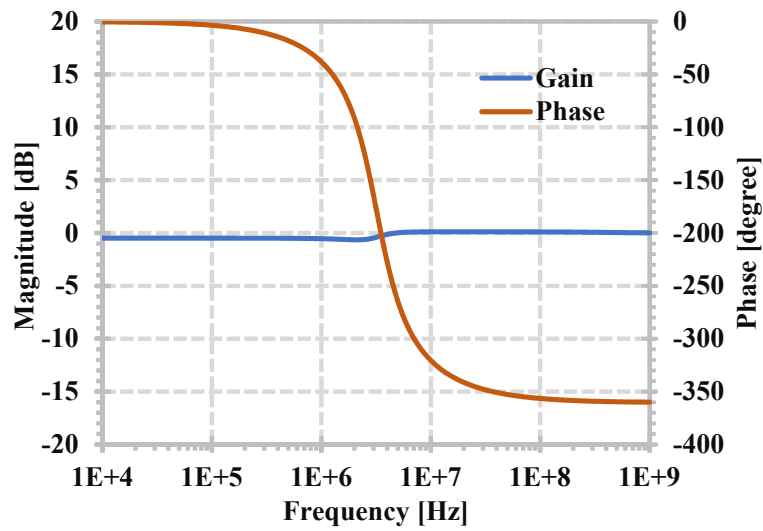

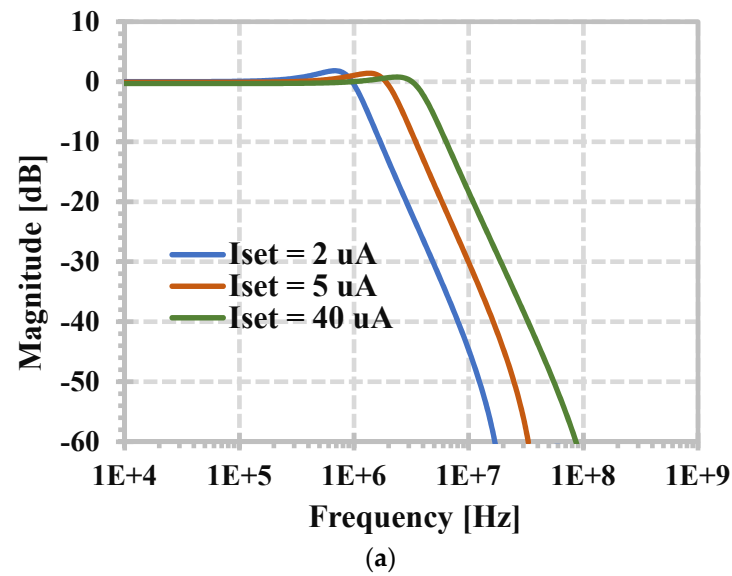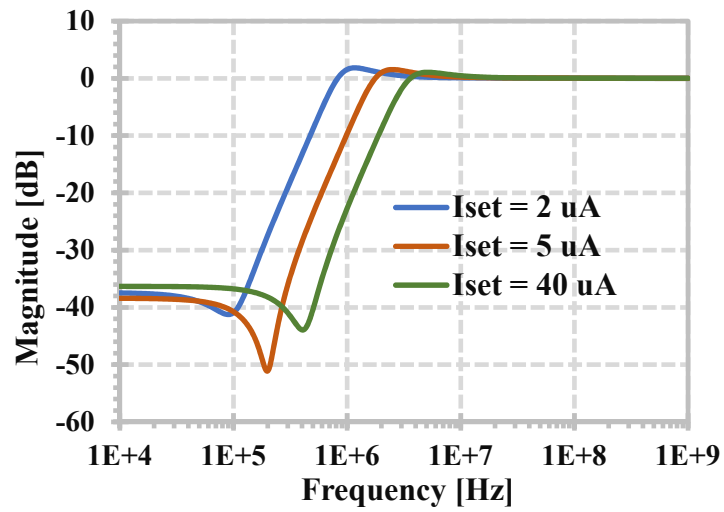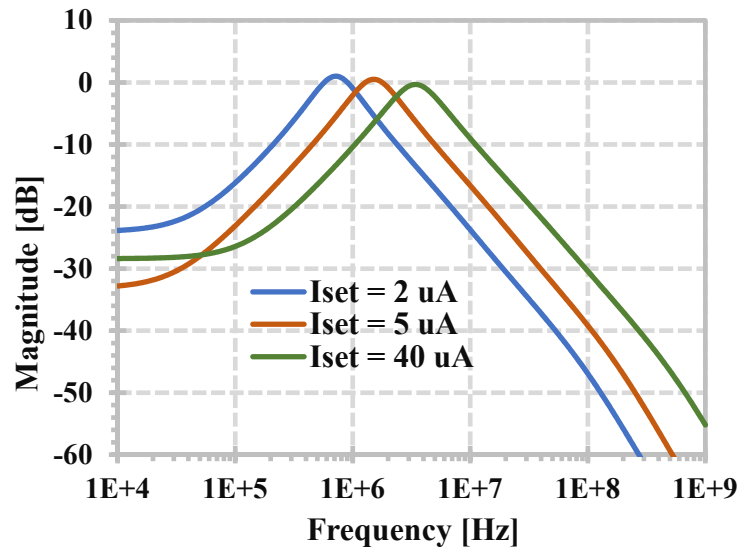**Figure 7.** Simulated magnitude and phase frequency responses of the APF.

(**a**)

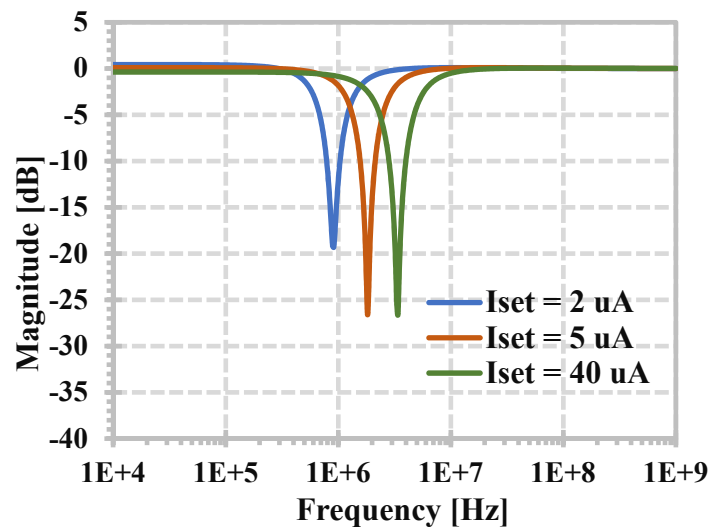**Figure 8.** *Cont*.

(b)

(c)

(d)

Figure 8. *Cont.*

(**e**)
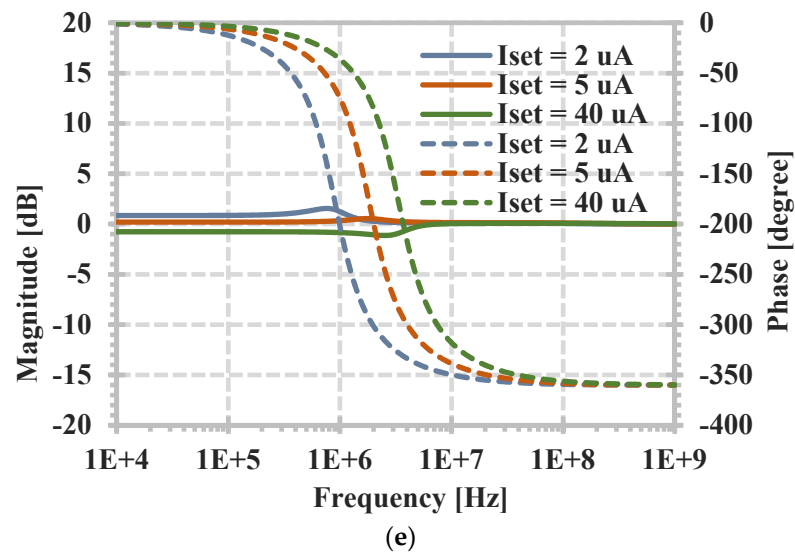
Figure 8. Simulated magnitude frequency responses with I_{set} = 2, 5, 40 µA, (**a**) LPF, (**b**) HPF, (**c**) BPF, (**d**) BSF, and (**e**) APF.
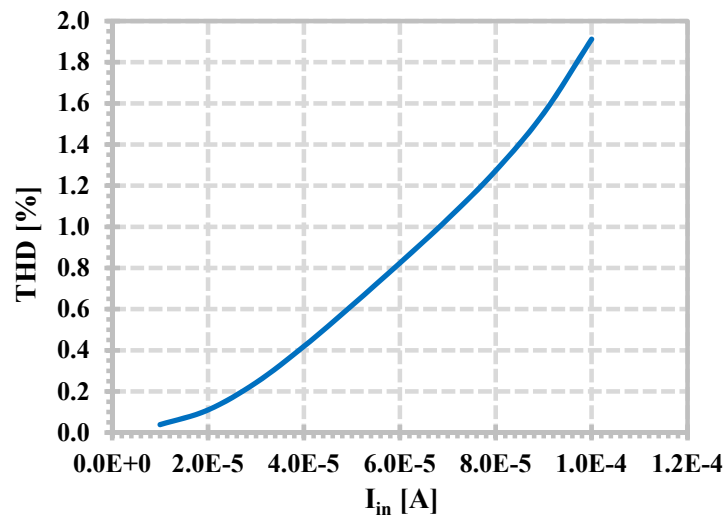

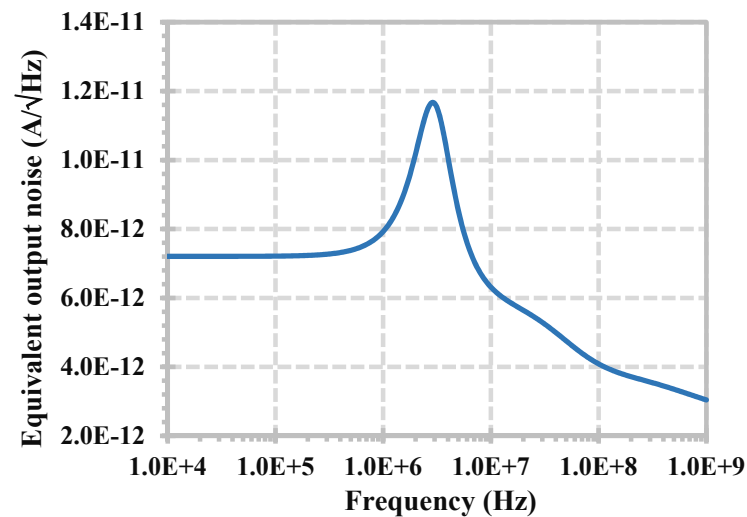**Figure 9.** Simulated THD of the LPF with different amplitudes of I_{in}.

Figure 10. The equivalent output current noise of the LPF.

Figure 11 shows the simulated frequency responses of the LPF, HPF, BPF, BSP, and APF when the temperature was set to −30, 27, and 85 °C. Figure 12 shows the simulated frequency responses of the filter when the voltage supply was set to 0.975 V, 1 V, and 1.25 V (1 V ± 5%). In both cases the curves overlapped or closed each other.

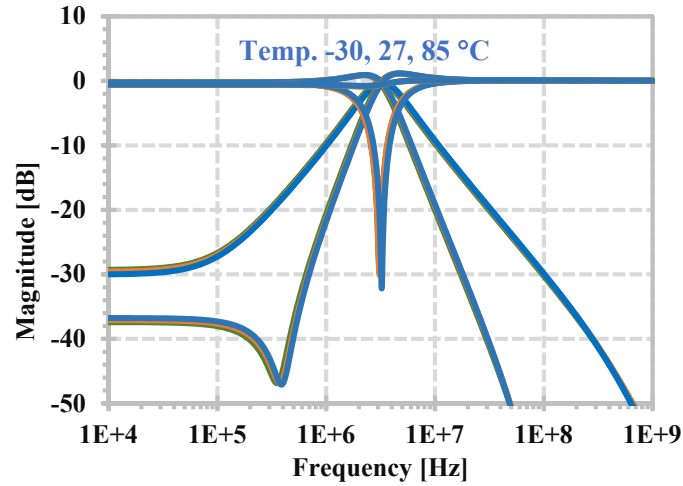**Figure 11.** The frequency response of the LPF, HPF, BPF, BSF, and APF with temperature corners.
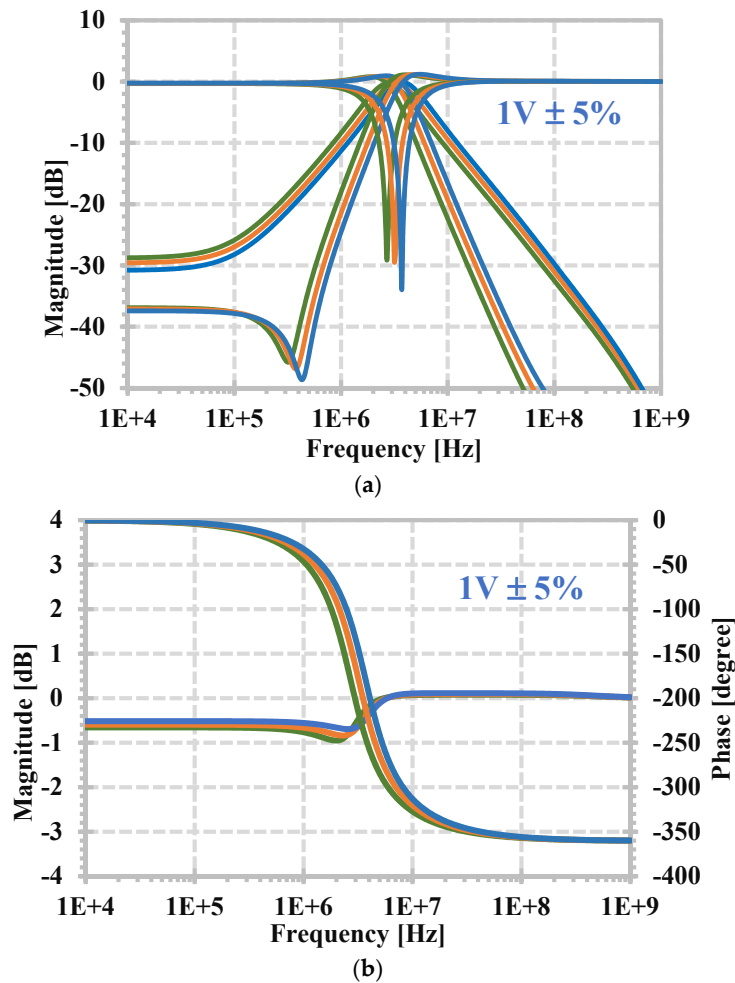

(**a**)

(**b**)

Figure 12. The frequency response of, (**a**) LPF, HPF, BPF, BSF, and (**b**) APF, with voltage supply corners.

Figure 13 shows the simulated magnitude frequency responses of the proposed filter when the threshold voltage in CMOS process was varied by 10% (LOT tolerance), which represents a process variation. As can be seen, the curves are closed to each other.
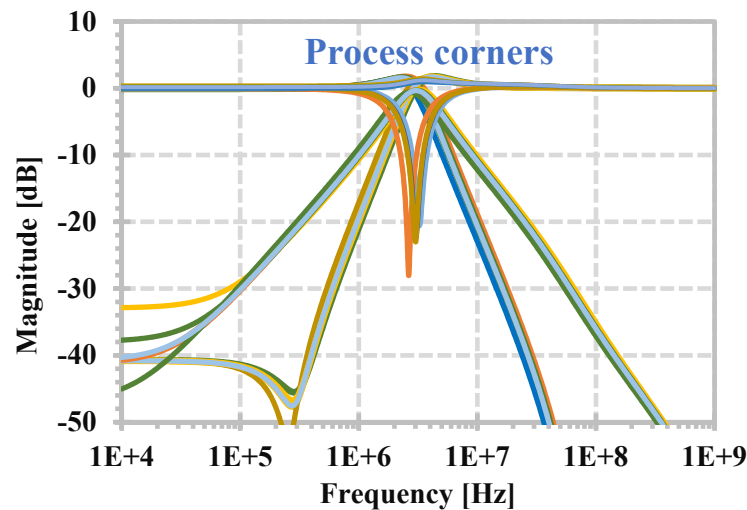

Figure 13. Simulated magnitude responses of the proposed filter for process corners.

The proposed current-mode filter was compared with previous works, as shown in Table 4. The current-mode filters that use similar active devices, such as VD-EXCCCII [18], EX-CCCII in [31,32], and DV-EXCCCII in [33,34], were used for comparison. Compared with [31–34], the proposed current-mode filter can realize LPF, HPF, BPF, BSF, and APF without inverted and double input signal conditions. Compared with [18], the proposed current-mode filter uses an EX-CCCII of a lower complexity than the VD-EXCCII. However, the VD-EXCCII based filter in [18] can offer mixed-mode operation (i.e., VM, CM, TAM, TIM), but two resistors are required. Moreover, for the filter in [18], it is difficult to tune the natural frequency because the equation of natural frequency includes both parameters of the transconductance g_m and resistance R. Thus, to tune the natural frequency without changing the quality factor, the condition $g_m = 1/R$ should be met.

Table 4. Comparison of this work with selected analog filters.

Factor	Proposed	[18]	[31]	[32]	[33]	[34]
Number of active devices	1-EX-CCCII	1-VD-EXCCII (Figure 4)	1-EX-CCCII (Figure 3)	1-EX-CCCII	1-DV-EXCCCII	1-DV-EXCCCII
Realization	CMOS structure and commercial IC	CMOS structure	CMOS structure	CMOS structure and commercial IC	CMOS structure and commercial IC	CMOS structure
Number of passive elements	2-C	2-C, 2-R	2-C	2-C	2-C	2-C, 1-R
Type of filter	MIMO	SIMO	MISO	MIMO	MISO	MISO
Operation mode	CM	CM	CM	MM	CM	CM
Number of offered responses	7	5	5	5 (CM)	5	5
All grounded capacitors	Yes	Yes	Yes	Yes (CM)	Yes	Yes

Table 4. *Cont.*

Factor	Proposed	[18]	[31]	[32]	[33]	[34]
Without inverted/double input conditions	Yes	Yes	No	No	No	No
High output impedances	Yes	Yes	Yes	Yes	Yes	Yes
Electronic control of ω_o	Yes	Yes	Yes	Yes	Yes	Yes
Voltage supply (V)	± 0.5	± 1.25	± 1.25	± 0.5	± 0.9	± 0.9
Natural frequency (MHz)	3.31	8.04	3.93	23	3.9	~3.5–4.2
Power dissipation (mW)	0.465	5.76	3.18	1.35	205	2.2
Total harmonic distortion (%)	1.038@140 μA_{pp}	2.5%@360 μA_{pp}	1.122%@100 μA_{pp} (BP)	0.2%@200 μA_{pp}	<6%@200 μA_{pp}	5%@120 μA_{pp} (BP)
Verification	Sim/Exp	Sim/Exp	Sim	Sim/Exp	Sim/Exp	Sim

4. Experimental Results

The EX-CCCII implementation used in this section to implement the current-mode universal filter is shown in Figure 14. The circuit is based on AD844 ICs and resistors. The resistors in the circuit are set as $R_1 = R_2 = R_3 = R_4$ to obtain $I_{x1} = I_{z1+} = -I_{z1-}$ and $R_{1c} = R_{2c} = R_{3c} = R_{4c}$ to obtain $I_{x2} = I_{z2+} = -I_{z2-}$. In this test, the resistors R_1, R_2, R_3, R_4, R_{1c}, R_{2c}, R_{3c}, and R_{4c} were 1 kΩ. The resistors R_{x1} and R_{x2} work as parasitic resistors of the EX-CCCII. The voltage-to-current (V/I) converter using AD844 and a resistor is used to convert the input voltage from a function generator to current inputs I_{in} (i.e., I_1, I_2, I_3, and I_4) ($I_{in} = V_{in}/R_{in}$), the example case for converting the voltage V_{in} to the input I_1 (I_{in}) was shown in Figure 14. To measure the output currents, i.e., I_{o1}, I_{o2}, I_{o3}, the current-to-voltage (I/V) converters are used ($V_{out} = I_{out}R_{out}$), Figure 14 shows the example case for converting the current I_{o3} (I_{out}) to the output V_{out}. In this test, the resistors R_{in} and R_{out} were 10 kΩ. Thus, a unity voltage gain was obtained. Figure 15 shows a photo of the experimental setup. The circuits were supplied from ± 5 V and 22-nF capacitances C_1 and C_2 were used. The measurement was performed using a Keysight DSOX1204G oscilloscope with a built-in signal generator.

Figure 16a,b show the measured magnitude responses of the LPF, HPF, BPF, BSP, and APF with setting resistances $R_{x1} = R_{x2} = 5$ kΩ. The measured natural frequency was 1.343 kHz while the filter was designed for a natural frequency of 1.446 kHz, giving an error of 7.12%. This result confirms the workability of the proposed current-mode filter.

Figure 17 shows the measured magnitude responses of the BPF when the resistances R_{x1} and R_{x2} ($R_{x1} = R_{x2}$) are set to 15 kΩ (a), 10 kΩ (b), 5 kΩ (c), and 1 kΩ (d). From (6) and (7), the natural frequency can be determined using $R_{x1} = R_{x2}$ while the quality factor (Q) can be selected using C_1/C_2. The capacitor values were fixed as $C_1 = C_2 = 22$ nF and the resistors $R_{x1} = R_{x2}$ are given, resulting in Q = 1. By setting the resistor's values from 15 kΩ, 10 kΩ, 5 kΩ, and 1 kΩ, the measured natural frequencies were found to be 0.469 kHz, 0.704 kHz, 1.343 kHz, and 6.668 kHz, respectively. The filter is designed for natural frequencies of 0.482 kHz, 0.723 kHz, 1.446 kHz, and 7.234 kHz, respectively. Thus, the errors were 2.69%, 2.62%, 7.12%, and 7.82%, respectively. This experimentation serves to confirm the tuning capability of the current-mode filter expressed in (6).
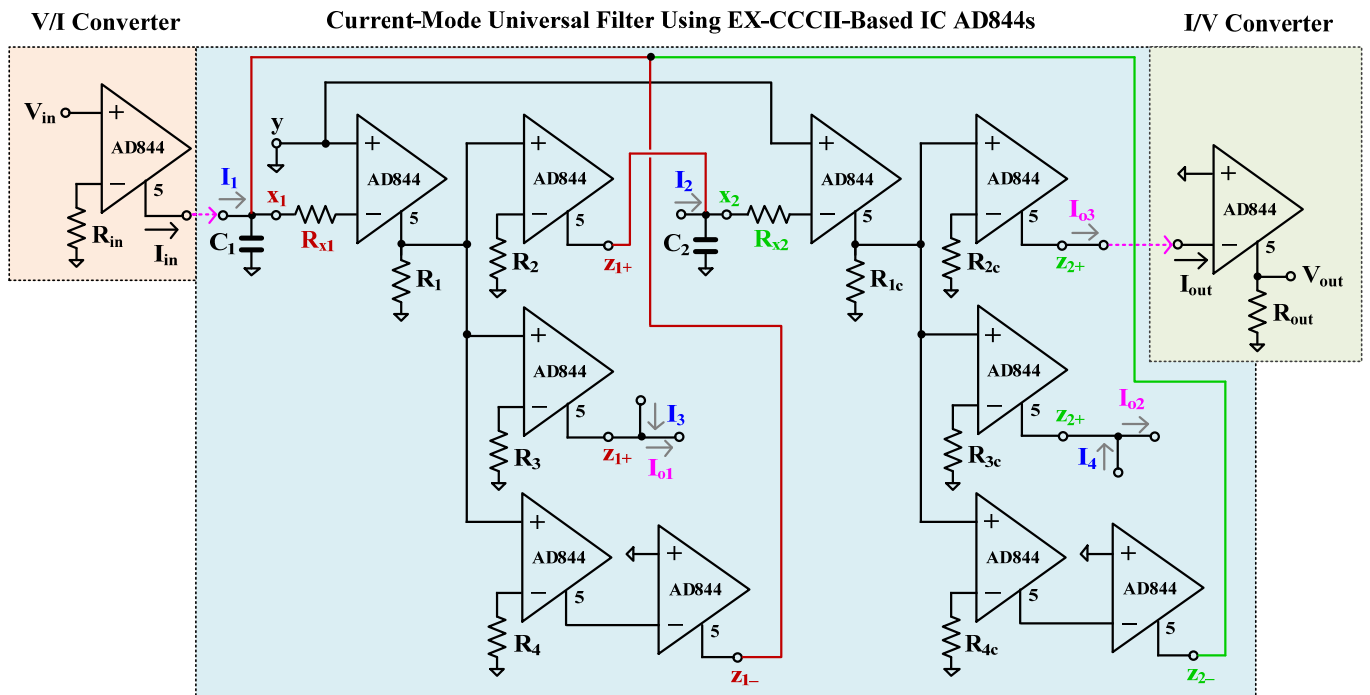
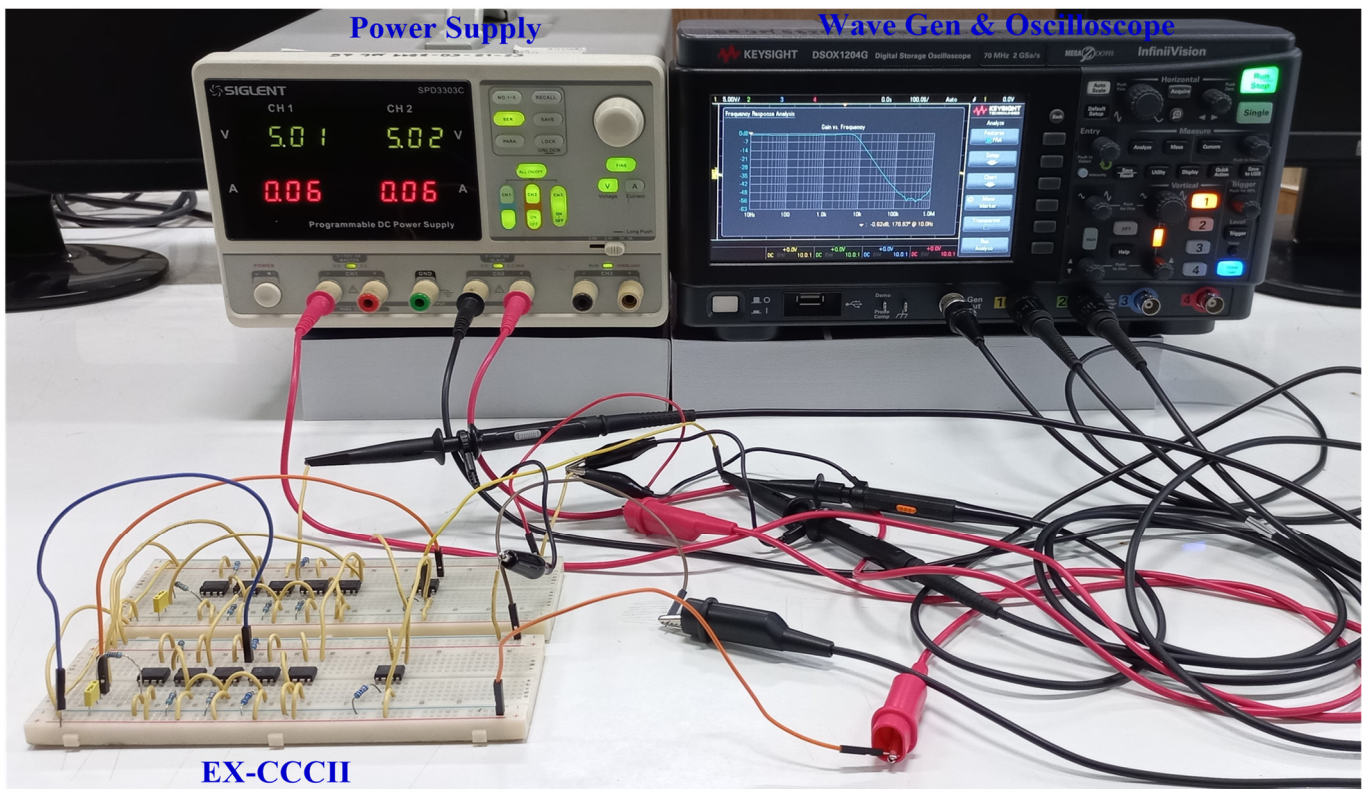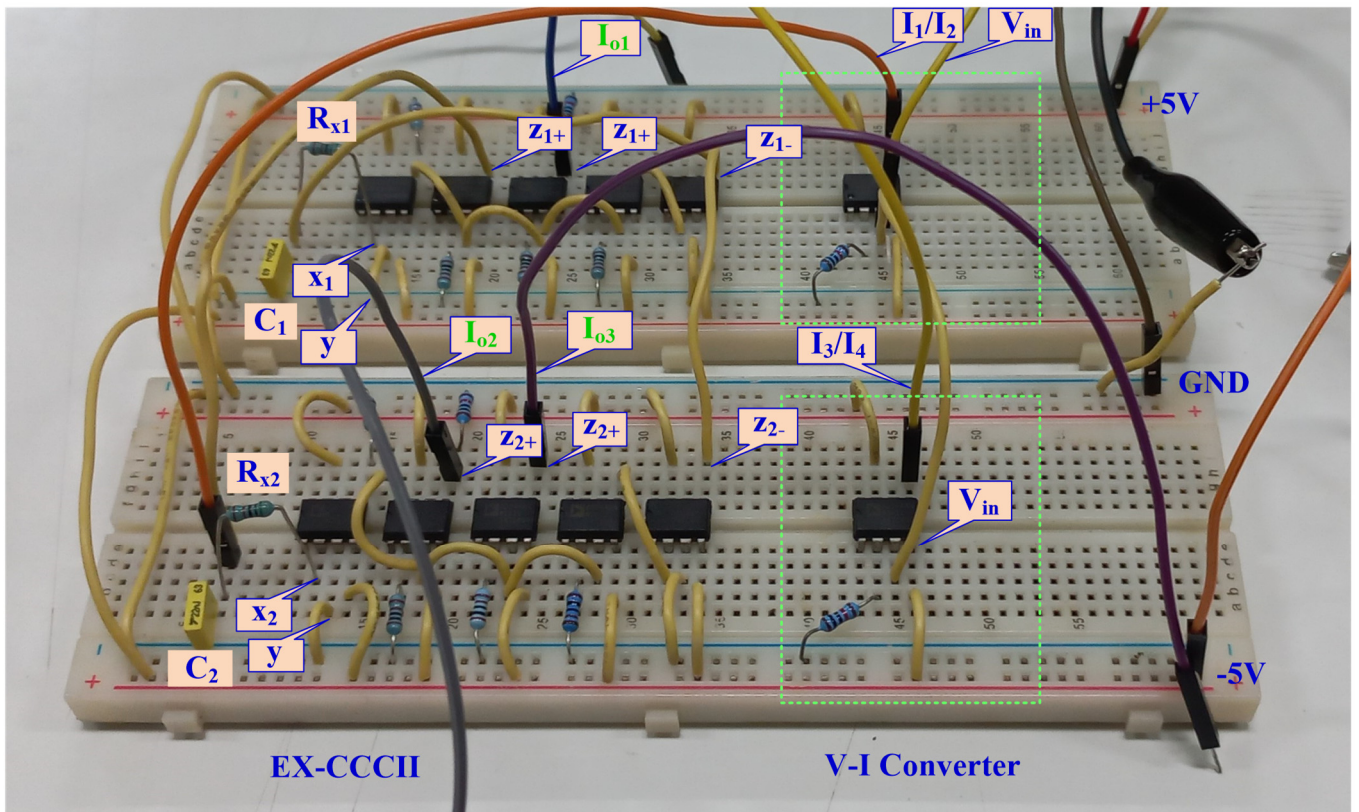**Figure 14.** Implementation of the EX-CCCII using AD844s to realize the current-mode universal filter.

(**a**)

Figure 15. *Cont*.

(**b**)

Figure 15. (**a**) Experimental setup, (**b**) close-up of the EX-CCCII and V/I converter.
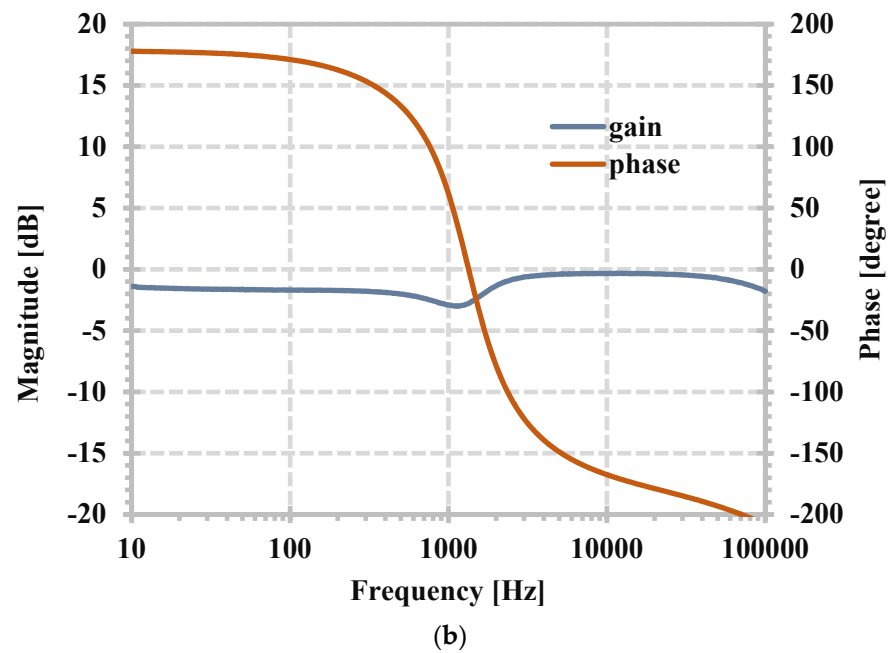

(**a**)

Figure 16. *Cont.*

(**b**)
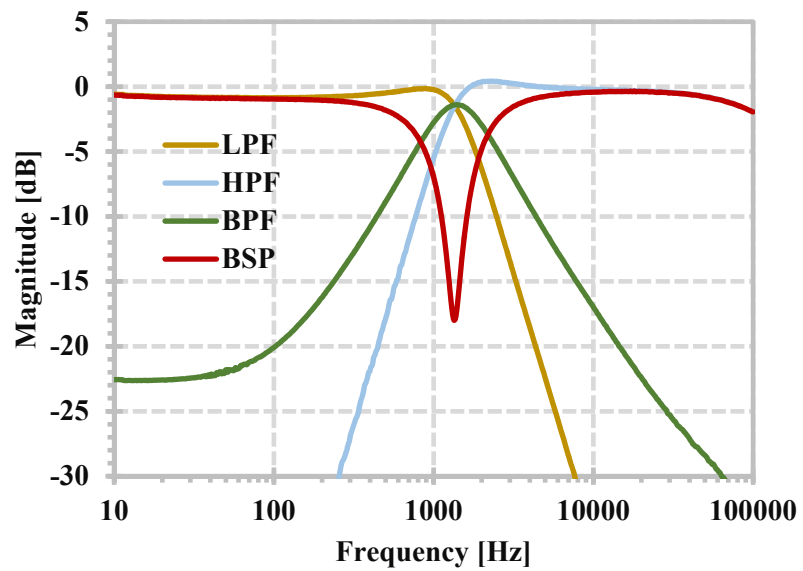
Figure 16. Magnitude responses with setting resistances $R_{x1} = R_{x2} = 5$ kΩ for (**a**) LPF, HPF BPF, BSF, and (**b**) APF.

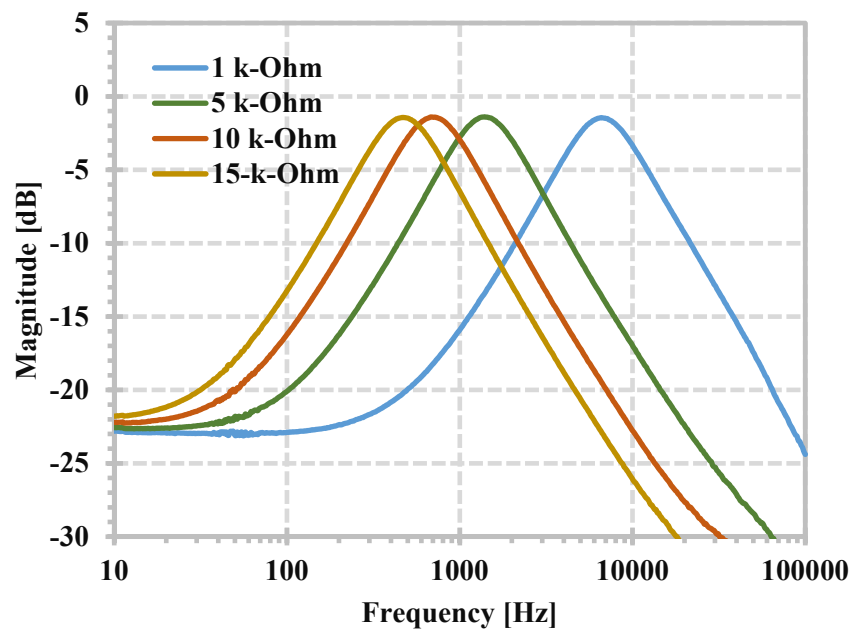**Figure 17.** Measured magnitude frequency responses of the BPF with setting resistances $R_{x1} = R_{x2}$ for (1, 5, 10, 15) kΩ.

5. Conclusions

In this study, a new electronically tunable current-mode universal analog filter with multiple inputs and multiple outputs is proposed. The filter employs only one EX-CCCII and two grounded capacitors. The topology can realize five standard filtering functions of low-pass, high-pass, band-pass, band-stop, and all-pass responses without changing the internal configuration of the filter by selecting the appropriate input and output signals. The inverted input signal and input matching conditions are absent for obtaining these filtering functions. The natural frequency of all filter responses can be electronically controlled. The

proposed filter was simulated by SPICE and confirmed through experimental testing using IC AD844s.

Author Contributions: Conceptualization, M.K., F.K. and T.K.; methodology, M.K., F.K. and T.K.; software, M.K. and F.K.; validation, M.K., F.K. and S.T.; formal analysis, M.K. and T.K.; investigation, M.K., F.K. and T.K.; resources, M.K.; data curation, M.K. and F.K.; writing—original draft preparation, M.K., F.K., T.K. and S.T.; writing—review and editing, M.K., F.K., T.K. and S.T.; visualization, M.K. and F.K.; supervision, M.K. and F.K.; project administration, M.K. and F.K.; funding acquisition, M.K. All authors have read and agreed to the published version of the manuscript.

Data Availability Statement: Data are contained within the article.

Conflicts of Interest: The authors declare no conflicts of interest.

References

1. Roberts, G.; Sedra, A. All current-mode frequency selective circuits. *Electron. Lett.* **1989**, *25*, 759–761. [CrossRef]
2. Toumazou, C.; Lidgey, F.J.; Haig, D.G. *Analogue IC Design: The Current-Mode Approach*; Peter Peregrinus: London, UK, 1990.
3. Sedra, A.; Smith, K. A second-generation current conveyor and its applications. *IEEE Trans. Circuit Theory* **1970**, *17*, 132–134. [CrossRef]
4. Fabre, A.; Saaid, O.; Wiest, F.; Boucheron, C. Current controlled bandpass filter based on translinear conveyors. *Electron. Lett.* **1995**, *31*, 1727–1728. [CrossRef]
5. Maheshwari, S. Current conveyor all-pass sections: Brief review and novel solution. *Sci. World J.* **2013**, *2013*, 429391. [CrossRef] [PubMed]
6. Maheshwari, S. Voltage-mode full-wave precision rectifier and an extended application as ASK/BPSK Circuit Using a Single EXCCII. *Int. J. Electron. Commun.* **2018**, *84*, 234–241. [CrossRef]
7. Maheshwari, S. Realization of simple electronic functions using EXCCII. *J. Circuits Syst. Comput.* **2017**, *26*, 1750171. [CrossRef]
8. Agrawal, D.; Maheshwari, S. Current-mode precision full-wave rectifier circuits. *Circuits Syst. Signal Process.* **2017**, *36*, 4293–4308. [CrossRef]
9. Das, R.; Paul, S.K. Resistorless current mode precision rectifier using EXCCII. *Analog. Integr. Circuits Signal Process.* **2020**, *103*, 511–522. [CrossRef]
10. Kapoulea, S.; Psychalinos, C.; Elwakil, A.S. Single active element implementation of fractional-order differentiators and integrators. *Int. J. Electron. Commun.* **2018**, *97*, 6–15. [CrossRef]
11. George, M.A.; Bhavani, I.V.L.D.; Kamath, D.V. EX-CCII Based FOPID controller for electric vehicle speed control. In Proceedings of the 2020 IEEE International Conference on Distributed Computing, VLSI, Electrical Circuits and Robotics (DISCOVER), Udupi, India, 30–31 October 2020; pp. 47–51.
12. Joshana, R.; Singh, Y.S.; Ranjan, A. An electronically tunable fractional order inductor employing VD-EXCCII. *Int. J. Electron. Commun.* **2023**, *174*, 155055. [CrossRef]
13. Agrawal, D.; Maheshwari, S. Design and implementation of current mode circuit for digital modulation. *Integration* **2021**, *78*, 118–123. [CrossRef]
14. Kumar, A. Single EXCCII-based analog multiplier structure. *J. Circuits Syst. Comput.* **2021**, *30*, 2150107. [CrossRef]
15. Chaturvedi, B.; Kumar, A. Single EXCCII based square/triangular wave generator for capacitive sensor interfacing and brief review. *VLSI Post-CMOS Electron. Devices Circuits Interconnects* **2019**, *2*, 329–349. [CrossRef]
16. Maheshwari, S.; Agrawal, D. High performance voltage-mode tunable all-pass section. *J. Circuits Syst. Comput.* **2015**, *24*, 1550082. [CrossRef]
17. Maheshwari, S. Tuning approach for first-order filters and new current-mode circuit example. *IET Circuits Devices Syst.* **2018**, *12*, 478–485. [CrossRef]
18. Faseehuddin, M.; Herencsar, N.; Albrni, M.A.; Sampe, J. Electronically tunable mixed-mode universal filter employing a single active block and a minimum number of passive components. *Appl. Sci.* **2021**, *11*, 55. [CrossRef]
19. Agrawal, D.; Maheshwari, S. Electronically tunable mixed-mode third-order universal filter using a single EX-CCII. *Aust. J. Electr. Electron. Eng.* **2022**, *19*, 307–323. [CrossRef]
20. Banerjee, K.; Joshi, M.; Sarkar, C.; Biring, S. Low-frequency resistorless electronically tunable quadrature oscillator based on an EX-CCII. *J. Electron. Mater.* **2023**, *52*, 1–6. [CrossRef]
21. Kumari, A.; Ranjan, A. Extra-X current controlled current conveyor based resistorless current mode quadrature sinusoidal oscillator. *Int. J. Appl. Eng. Res.* **2018**, *13*, 1–5.
22. Bhatt, V.; Ranjan, A.; Singh, Y.S. Resistorless Chua's diode implementation for chaotic oscillation employing single EXCCII. *Int. J. Electron. Commun.* **2022**, *156*, 154398. [CrossRef]

23. Li, Y.; Hou, J. Pathological models of EXCCCII and its applications in oscillator synthesis. *Wuhan Univ. J. Nat. Sci.* **2022**, *26*, 115–122. [CrossRef]

24. Singh, P.; Nagaria, R.K. Single EX-CCCII based electronically tunable current mode instrumentation amplifier. *Eng. Rev.* **2022**, *42*, 1–16. [CrossRef]

25. Agrawal, D.; Maheshwari, S. Cascadable current mode instrumentation amplifier. *Int. J. Electron. Commun.* **2018**, *94*, 91–101. [CrossRef]

26. Agrawal, D. Electronically Tunable Grounded Immittance Simulators Using an EX-CCCII. *Int. J. Electron.* **2020**, *107*, 1625–1648. [CrossRef]

27. Singh, P.; Nagaria, R. Low voltage EX-CCCII based on quasi-floating gate technique and its application as precision rectifier. *Int. J. Electron. Commun.* **2022**, *155*, 154378. [CrossRef]

28. Singh, P.; Varshney, V.; Kumar, A.; Nagaria, R.K. DV-EXCCCII–based electronically tunable voltage mode all-pass filter. *Lect. Notes Electr. Eng.* **2021**, *777*, 485–494. [CrossRef] [PubMed]

29. Maheshwari, S.; Agrawal, D. Cascadable and tunable analog building blocks using EX-CCCII. *J. Circuits Syst. Comput.* **2017**, *26*, 1750093. [CrossRef]

30. Singh, P.; Varshney, V.; Kumar, A.; Nagaria, R.K. DV-EXCCCII–based electronically tunable current mode filter. *Lect. Notes Electr. Eng.* **2021**, *777*, 235–245. [CrossRef] [PubMed]

31. Agrawal, D.; Maheshwari, S. Current mode filters with reduced complexity using a single EX-CCCII. *Int. J. Electron. Commun.* **2017**, *80*, 86–93. [CrossRef]

32. Agrawal, D.; Maheshwari, S. High-performance electronically tunable analog filter using a single EX-CCCII. *Circuits Syst. Signal Process.* **2021**, *40*, 1127–1151. [CrossRef]

33. Singh, P.; Nagaria, R.K. DV-EXCCCII based resistor-less current-mode universal biquadratic filter. *Adv. Technol. Innov.* **2023**, *8*, 12–28. [CrossRef]

34. Singh, P.; Nagaria, R.K. Electronically tunable DV-EXCCCII-based universal filter. *Int. J. Electron. Lett.* **2020**, *9*, 301–317. [CrossRef]